

Adsorptive Behavior of Catechol Violet and Its Thorium Complex on Mercury Electrode in Aqueous Media

Mostafa K. M. Rabia[†]

Chemistry Department, Faculty of Science, South Valley University, Sohag, Egypt
(Received September 5, 2003 : Accepted November 14, 2003)

Abstract : Cyclic voltammetry and chronocoulometry have been used for characterization of catechol violet (CV) at the hanging mercury drop electrode in acetic acid-sodium acetate buffer solution. At pH 2.94 a nearly symmetric cyclic voltammetric wave due to an irreversible weak adsorption of CV on mercury was obtained at concentration of $0.53 \mu\text{mol dm}^{-3}$. Under these conditions, CV adsorbs in a monolayer. Upon increasing the concentration, the symmetry of the wave decreases; it can be attributed to a mixed diffusion adsorption process. The amount of the adsorbed catechol violet on the HMDE expressed as surface concentration as well as the surface areas occupied by one molecule (σ) were calculated. It was found that the values obtained for Γ and σ utilizing cyclic voltammetric and chronocoulometry are almost identical. A 1:1 and 1:2 Th (IV)-CV complexes are formed on addition of thorium (IV) to catechol violet. These complexes are adsorbed and reduced on the HMDE at more negative potentials than the peak potential of free CV. Using the square-wave (SW) technique, the adsorptive cathodic stripping voltammetry, ACSV, of these complexes was studied. It was found that the SW-ACSV of Th(IV)-CV can be applied to the determination of thorium at the nanomole level. Optimum conditions and the analytical method of determination were presented and discussed.

Key words : Catechol violet, Adsorption, Thorium complex, Cyclic voltammetry, Chronocoulometry, Stripping voltammetric determination.

1. Introduction

The electrochemical behaviour of catechol violet is important due to its use as a metallochromic indicator,¹⁻⁴⁾ in spectrophotometric trace measurements of metal ions,⁵⁾ in flow injection spectrophotometry for trace elements in environmental⁶⁻⁸⁾ and food⁹⁾ analysis, in the stripping voltammetric trace analysis of titanium¹⁰⁾ as well as for application as a charge-transfer mediator in the oxidation of nicotinamide adenine dinucleotide (NADH).¹¹⁾ Thus, in continuation of our laboratory previous work on sulfonephthaleins¹²⁻¹⁴⁾ it seems of interest to study the adsorption behaviour of the title compound.

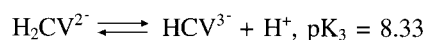
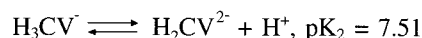
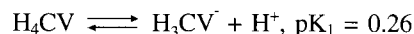
A previous publication¹²⁾ presented the electrochemical reduction mechanism of catechol violet. It shows a single diffusion-controlled two-electron cyclic voltammetric wave at lower pH (< 7) and the reduction pathway follows an ECEC, first-order kinetics. At higher pH, two diffusion-controlled monoelectronic cyclic voltammetric waves were seen and the reduction proceeds via an EEC, first-order process.

One purpose of the present investigation is to establish a complete characterization of the adsorption behaviour of catechol violet at the hanging mercury drop electrode (HMDE) in aqueous acetate buffer solutions at different pH's. Various electrochemical techniques were used: cyclic voltammetry and double potential step chronoamperometry and chronocoulom-

etry, which are powerful for a quantitative characterization of the adsorption process. The second purpose is to study the adsorptive behaviour of the catechol violet-Th (IV) complex at the HMDE. Square-wave voltammetry was used for this study. The study is also extended to the analytical determination of Thorium(IV).

2. Results and Discussion

Catechol violet(CV), 3,3',4-trihydroxy-o-cresol-sulphonaphthalein, has the structural formula as shown below and is abbreviated as H₄CV. It provides four species,⁵⁾ H₄CV (highly acidic), H₃CV⁻ (pH=1-2), H₂CV²⁻ (pH=5-7), and HCV³⁻ (pH.8) according to the following equilibriums:



The equilibrium concentration of these species has been calculated¹⁵⁾ in the entire pH (1.68-10.94) from the knowledge of the analytical concentration, pK₂ and pK₃ values of CV along with the pH of the experimental solution.

Cyclic voltammetric behaviour of CV was investigated in aqueous buffer solutions at different pHs. It was suggested

[†]E-mail: mostafarabia@hotmail.com

earlier^{12,16,17}) that at lower pHs the reduction process of CV involves two electrons and two protons and follow an ECEC reduction mechanism giving a single two-electron diffusion-controlled cyclic voltammetric wave.

More intention will be given to explore the adsorption behaviour of CV in detail to obtain better insight into its electrochemical reduction. Herein, cyclic voltammetry and chronoamperometry or chronocoulometry are the methods of choice.

Cyclic voltammetry

Fig. 1 shows cyclic voltammograms of different concentrations of CV at scan rate, $\nu = 200 \text{ mV s}^{-1}$, at the hanging mercury drop electrode, HMDE. Representative voltammetric data are collected in Table 1. At slow scan rates ($\nu \leq 200 \text{ mV s}^{-1}$) the wave is irreversible, since its anodic counterpart is lacking. The shape of the wave suggests that it corresponds to a faradaic surface process. On increasing the scan rates ($\nu \geq 400 \text{ mV s}^{-1}$), an anodic wave is observed on the reversal scan. This anodic wave presumably indicates that no desorption process of the electroactive species takes place upon reduction. Straight lines ($r = 0.998$) obtained between $\log i_p$ and $\log \nu^{1/2}$ within the concentration range of $0.53\text{--}6.40 \mu\text{mol dm}^{-3}$ with slopes 0.89 ± 0.05 indicate that the cyclic voltammetric peak is due to a mixed diffusion adsorption process.

Using diagnostic criteria suggested previously^{19,20}) the voltammogram shows a symmetric shape at low concentration (0.53 to $6.40 \mu\text{mol dm}^{-3}$), whereas at higher concentrations ($>6.40 \mu\text{mol dm}^{-3}$) the symmetry is nearly lost. The symmetric appearance at lower concentration is indicative of adsorption (c.f. Fig. 1).

On plotting the current function ($i_p/C\nu^{1/2}$) vs. $\log \nu$, at low concentration of CV an increase in the scan rate causes an increase in the current function. This behaviour would be expected for a weak adsorption of the reactant.¹⁹⁾ At a certain scan rate ($\nu = 200 \text{ mV/s}$), the current function deviates from the constant value which would be expected for the uncomplicated diffusion wave caused by adsorption at higher concentrations. The largest deviations are observed at lower concentrations ($516, 497$ and $182 \text{ nA/mmol dm}^{-3} (\text{V/s})^{1/2}$ at $[\text{CV}] = 0.53, 1.07$ and $2.13 \mu\text{mol dm}^{-3}$, respectively). This can be interpreted on the basis that the adsorbed molecules

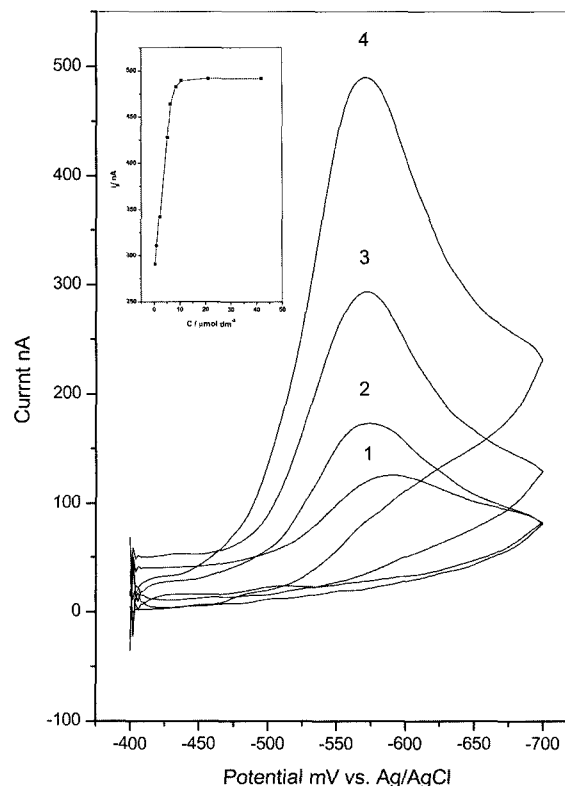


Fig. 1. Cyclic voltammograms of different concentrations of CV: 1) 5.55×10^{-7} , 2) 2.13×10^{-6} , 3) 5.33×10^{-6} , 4) $4.26 \times 10^{-5} \text{ mol dm}^{-3}$ (inset peak current variation with concentration) in acetic acid-sodium acetate buffer solution pH 2.94, at $\nu = 200 \text{ V s}^{-1}$.

of CV constitute a constant flow of matters and charge, whereas the amount of molecules diffusing to the electrode is time dependent. At sufficiently fast scan rates, the amount of diffusing molecules is small relative to that of the adsorbed ones; whereas at low scan rates, the opposite is true. Thus, an increase in the current function is observed with increasing scan rate.

The inset Figure (c.f. Fig. 1), relationship between peak current and concentration of CV, shows that the peak current increase linearly in the low concentrations range ($\leq 6.40 \mu\text{mol dm}^{-3}$). Further increase in concentration causes a marked non-linear influence on the peak current. This is ascribed to a nearly total coverage of the electrode surface as the con-

Table 1. Cyclic voltammetric data for $1.07 \mu\text{mol dm}^{-3}$ CV in an acetic acid-acetate buffer solution at pH 2.94.

ν (mV/s)	Forward			Backward		
	$-E_p$ (mV)	i_p (nA)	$i_p/C\nu^{1/2}$ nA/mm $\text{mol dm}^{-3} (\text{V/s})^{1/2}$	$-E_p$ (mV)	i_p (nA)	$i_p/C\nu^{1/2}$ nA/mm $\text{mol dm}^{-3} (\text{V/s})^{1/2}$
50	550	108	451	-	-	-
100	559	168	497	-	-	-
200	570	247	516	-	-	-
400	573	378	589	535	130	192
600	573	551	665	538	165	199
800	573	661	691	540	197	206
1000	573	869	812	543	319	298

centration is increased. The total current due to the reduction of the adsorbed molecules becomes constant, whereas the total current caused by the diffusing molecules continues to increase with increasing concentration. This results in a decrease of the fraction of the peak current due to adsorption with increasing concentration.

Examination of a plot of the current function vs. $\log C^*$ reveals that, the current function is low value at high concentrations. As the concentration is decreased, the current function increases and finally reaches a limiting value at low concentrations where its behaviour becomes independent of concentration. The increase in the current function is attributed to a decrease of the current due to diffusion species upon decreasing concentration, whereas the limiting value is due to the constant amount of adsorbate. This behaviour supports the above conclusion that the electrochemical response is due to a weak adsorption of CV.

The observed half width, $W_{1/2}$, for CV adsorption wave is 122.3 ± 11.3 mV. This value suggests the transfer of one electron for the irreversible redox couple of CV. The difference to the expected theoretical value ($90.6/n$ mV^{21,22}) is due to an irreversible adsorption of CV.

The shift of the adsorption wave at low concentrations to more negative potentials as the pH of the solution is increased, indicates the participation of protons in the electrochemical reduction process of the adsorbed species at the mercury electrode. The linear dependence of the peak potential on the pH value can be represented by eqn(1):

$$E_p = -0.336 - 0.075 \text{ pH} \quad r = 0.996 \quad (1)$$

The number of participating protons (ρ) in the adsorption process can be evaluated from the gradient of eqn.(1) by using equation (2)²³

$$\rho = (\Delta E_p / \Delta \text{pH}) \cdot (\alpha n_a / 0.059) \quad (2)$$

where n_a is the number of electrons involved in the adsorption process. It is evident from the slope value of eqn. (1) that one proton is consumed. Moreover, the slope of the adsorption wave is steeper than that expected for diffusion control. This reveals that the shift of the peak potential is not only due to the proton dependence of the redox reaction involving the adsorbed species, but also reflects a change in adsorption strength of the reduced form relative to that of the oxidized form with varying pH. The steeper slope for the adsorption strength of the reduced form decrease with increasing pH value.

The area of the cathodic wave for the voltammogram was calculated. It was found that the area of the adsorption wave depends on the substrate concentration, reaching a limiting value at higher concentrations. The amount of adsorbed catechol violet was determined from that area of the cathodic wave and expressed as the surface concentration (Γ , mol cm^{-2}) which is estimated using eqn(3).²²

$$A_{ad} = nFA \Gamma \quad (3)$$

where A_{ad} is the area of the adsorption peak, A is the electrode surface area and Γ is the surface concentration.

Fig. 2 shows the surface concentration (Γ) as a function of the negative logarithm of the substrate concentration shows an increase in the surface concentration upon increasing bulk concentration and then levels off at higher values; obviously, coverage and orientation are essentially monolayer and unchanged as the solute concentration is increased by two orders of magnitude.²⁴ This resistance to reorientation is probably due to interaction of the aromatic rings of CV with the electrode surface in a flat orientation which would permit only limited interaction. It can be seen from Fig. 2 that the surface coverage reaches saturation at 6.40×10^{-6} mol dm^{-3} CV. Increasing the concentration of CV above 6.40×10^{-6} mol dm^{-3} affects the shape of the waves; as the concentration of CV increases, the wave becomes sharper. Such changes are indicative of organization processes. It is evident that the relationships are reminiscent of a Langmuir isotherm, eqn. 3^{21,22}) is;

$$\Gamma_i / (\Gamma_{is} / \Gamma_i) = b_i c_i \quad (4)$$

where Γ_i is the surface concentration of the adsorbed species i , Γ_{is} is the surface excess at the maximum coverage, b_i is the adsorption coefficient, and c_i is the bulk concentration. It can be linearized in the following form:

$$c_i / \Gamma_i = 1 / \Gamma_{is} b_i + c_i / \Gamma_{is} \quad (5)$$

The linear least-square fit obtained for plotting. c_i / Γ_i against (c_i) can be represented by;

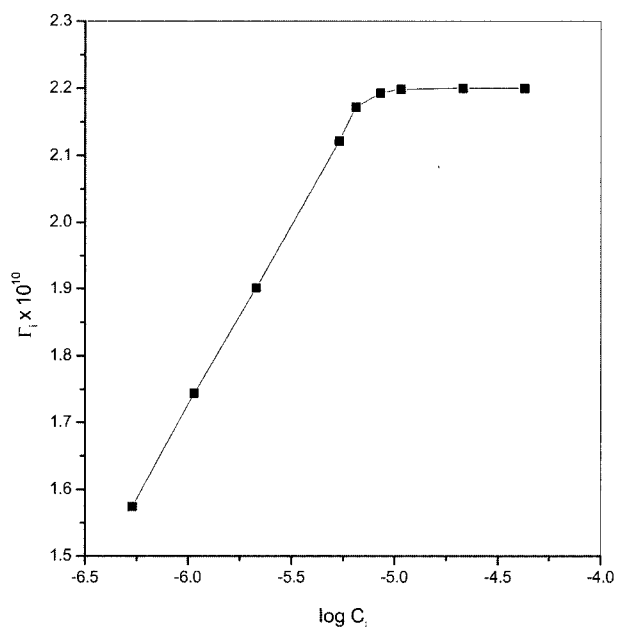


Fig. 2. A plot of surface concentration (Γ_i) against the negative logarithm of bulk concentration (C_i) at the same conditions cited in Fig. 1.

$$c_i/\Gamma_i = (1.47 \pm 0.03) \times 10^4 + (4.57 \pm 0.02) \times 10^9 c_i \quad (6)$$

($r = 0.995$)

The calculated value of Γ_{is} of the adsorbed product is found to be $(2.19 \times 10^{-10}) \text{ mol cm}^{-2}$, which is slightly lower than the above limiting value. The adsorption coefficient of the adsorbate (b_i) is estimated to be $(3.11 \pm 0.02) \times 10^5 \text{ mol}^{-1}$. The excess of surface coverage calculated under saturation conditions equals $(2.19 \times 10^{-10} \text{ mol cm}^{-2})$ which corresponds to 75.83 \AA^2 per molecule of CV. This means that a monolayer is formed on the surface.

Chronocoulometry

Double-potential step chronocoulometry provides a useful method for the quantitative characterization of an adsorption process independent of both the relative reduction potentials of the diffused and adsorbed species and the kinetics of their electrode reactions.²² In a particular double step chronocoulometric experiment, the potential is held at an initial value E_i where no electrolysis occurs and is rapidly stepped to a value E_f at which the desired electrode reaction takes at $t = 0$. At $t = \tau$, the potential is returned to E_i . The chronocoulometric data were analysed according to Ansons equations²⁵ (eqns. (7) and (8)):

$$Q(t < \tau) = \frac{2nFAD_o^{1/2}C_o t^{1/2}}{\pi^{1/2}} + Q_{dl} + nFAG \quad (7)$$

$$Q_r(t) = \frac{2nFAD_o^{1/2}C_o \theta}{\pi^{1/2}} + Q_{dl} \quad (8)$$

where $Q(t < \tau)$ is the amount of charge that has passed at time t since the application of the potential step, C_o and D_o are the concentration and diffusion coefficient of the reactants, respectively, A is the electrode surface, n and F have their usual significance, $Q_r(t) = Q(\tau) - Q(t > \tau)$, Q_{dl} is the charge consumed by the electrode-electrolyte double-layer capacitance, Γ_{is} the excess surface of the adsorbate, and $\theta = (\tau^{1/2} + (t-\tau)^{1/2})^2 t^{1/2}$.

In solutions of low pH values (2.94), the electrode potential was stepped from an initial value $E_i = -0.45 \text{ V}$, where CV is electrochemically inactive, to a final value $E_f = -0.60 \text{ V}$ where the electrode reaction proceeds. The potential was held at E_f for a time τ at which it was stepped back to E_i and maintained there for the same time interval. The charge that passes through the electrode during each of the time intervals was measured.

Plots of $Q_f(t < \tau)$ vs. $t^{1/2}$ according to eqn.(7) and $Q_r(t > \tau)$ vs. θ according to Eqn.(8) affords good straight lines for the entire time range (correlation coefficients: 0.999 and 0.997; cf. Fig. 3 as representative example). They have different slopes and intersect each other above the t -axis. This demonstrates the adsorption of the subject compound on the electrode surface. According to eqn.(7), the diffusion coefficient of CV calculated from the slope is $4.5 \times 10^{-6} \text{ cm}^2/\text{sec}$. On the other hand, the intercept is larger than that obtained for the

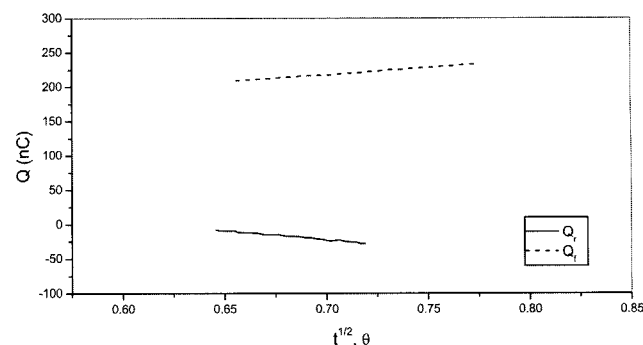


Fig. 3. Anson plots of Q_f vs. $t^{1/2}$ and Q_r vs. θ for $2.07 \mu\text{mol dm}^{-3}$ CV at the same conditions cited in Fig. 1.

quantity of electricity needed to charge the electrode electrolyte double layer of the supporting electrolyte ($Q_{dl} = 2.6 \text{ nC}$). This indicates the presence of adsorption in addition to the diffusion process. Furthermore, the amount of the adsorbate is determined from the difference in intercepts for the forward and reverse Anson plots (eqns. (7) and (8)). The charge obtained for a concentration of $6.40 \mu\text{mol dm}^{-3}$ CV is found to be 3.75 nC/cm^2 which is equivalent to a surface excess of $2.35 \times 10^{-10} \text{ mol/cm}^2$. On increasing concentration of CV to $42.65 \mu\text{mol dm}^{-3}$, the computed surface excess of Γ increase to $2.6 \times 10^{-10} \text{ mol/cm}^2$.

Finally, the surface area of the electrode occupied by one molecule, σ , can be estimated from $\sigma = 1/N_L\Gamma$, where N_L is Loschmidt's number and Γ is the surface concentration in mol/\AA^2 . Examination of Fig. 2 shows that the limiting coverage value is attained at a bulk concentration of $6.40 \mu\text{mol dm}^{-3}$ catechol violet. Thus, the surface area occupied by the adsorbed substrate molecules can be calculated from the value of surface concentration at $6.40 \mu\text{mol dm}^{-3}$ to be 70.09 \AA^2 . It is evident that the values of both Γ and σ from cyclic voltammetry and chronocoulometric techniques are almost identical.

Thorium(IV) Catechol Violet

Free catechol violet (CV) as well as Th(IV)-CV complexes were found to adsorb onto a hanging mercury drop electrode (HMDE). Fig. 4 shows some square wave (SW) voltammograms of $2.07 \times 10^{-6} \text{ mol dm}^{-3}$ CV spikes with concentrations of Th(IV) varying from 0 to 3.0 molar ratio, Th(IV)-CV, in a 0.1 mol dm^{-3} acetate/ 0.1 mol dm^{-3} sodium perchlorate aqueous solution at pH 4.04. This figure exhibits three irreversible reduction waves in the entire potential range, -0.35 to -0.95 V , with peak potentials of -0.630 , -0.672 and -0.750 V . The first peak attributed to the reduction of the uncomplexed CV, since it is located at the peak potential of the free CV. The other two waves are due to the reduction of the Th(IV)-CV complexes, since the reduction wave of CV is shifted to more negative potentials on complexation with Th(IV). A very significant enhancement of the voltammetric response was achieved after adsorption of electroactive species onto a HMDE. Addition of Th(IV) to the CV solution resulted in a decrease in the peak current for CV reduction wave and

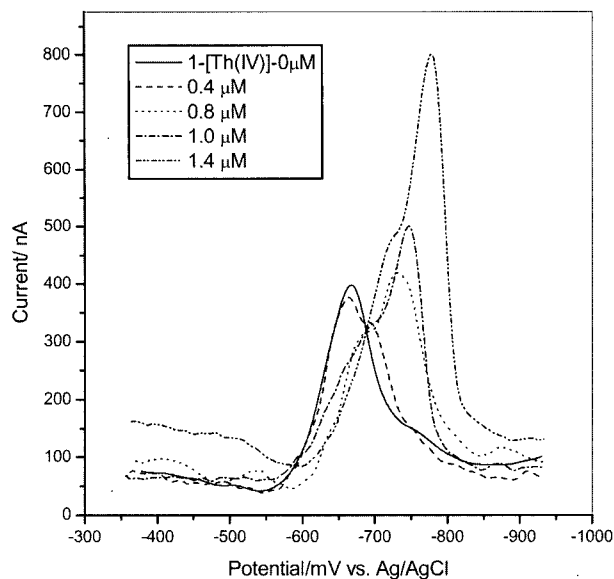


Fig. 4. Square-wave voltammograms of $2.07 \mu\text{mol dm}^{-3}$ CV containing different concentrations of Th(IV) in 20 mmol dm^{-3} acetic acid-acetate/ 0.1 M NaClO_4 buffer solution, pH 4.04. Preconcentration time 30 s, frequency 100 Hz.

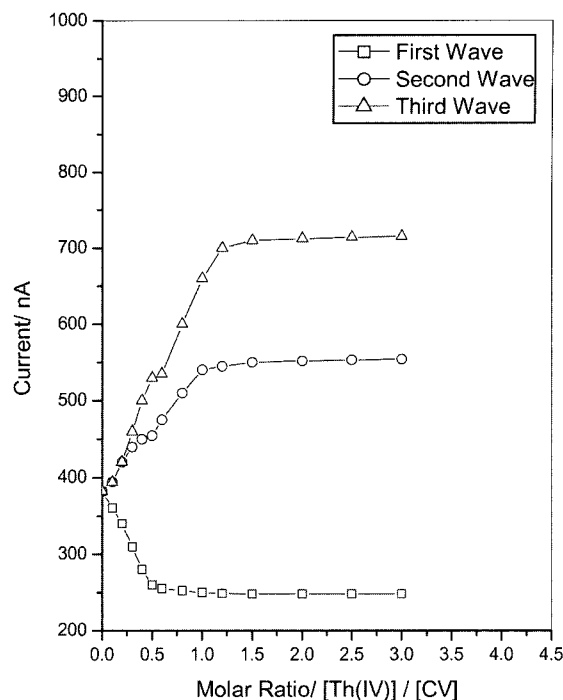


Fig. 5. Variation of peak current with mole ratio of Th(IV) for Th-CV system at the conditions cited in Fig. 4 for the three waves.

development (with increasing the peak current) of a second wave at more negative potentials for Th(IV)-CV complex. On increasing the concentration of Th(IV), the first wave is further decrease and the second one is grows while the third wave tends to develop at molar ratio ~ 0.3 and it grows with further increase in the molar ratio of Th(IV). The plotting of the peak current versus molar ratio, $[M]:[L]$, was used for determination of the composition of the metal complexes.²⁶⁻²⁸⁾ The results are shown in Fig. 5. This figure shows that the peak current for free CV, the first wave, decreases on increasing the mole ratio of Th(IV), reaching a more or less constant value at the 0.5 mole ratio. This is indicative of formation of a complex with a composition of 1:2 Th(IV):CV, under such conditions. This ratio has also reported by Jarosz.²⁹⁾ For the second wave, the peak current increases on increasing the mole ratio $[\text{Th(IV)}]/[\text{CV}]$ and levels off at a molar ratio of 1.0. The curve has two breaks at molar ratios of 0.5 and 1.0 which are due to the change of the composition of the reducible species. This indicates the formation of two complex species of 1:2 and 1:1 composition (Th(IV):CV). Furthermore, the stoichiometric ratios of 1:2 and 1:1 (Th(IV):CV) are also evident at the third wave (c.f. Fig. 5). This emphasizes the composition suggested from the data at the first and the second waves.

Catechol violet is a member of a class of sulfonephthalein (triphenylmethane series) compounds. It has four hydroxy chelating groups, two on each catechol ring. Thus the donor atoms in the CV molecule are four hydroxy oxygens. At the given pH, 4.04, CV exists in the H_3CV^- form, which with subsequent elimination of a proton, reacts with Th(IV) to form Th(IV)-CV complexes of the composition of 1:1 and 1:2. This behaviour is indicative from a quite different of the cyclic and square-wave voltammetry corresponding to the

complexes from those of the free CV. Complexes with a single metal ion coordinated to one and two CV groups have been reported.³⁰⁾

With increasing solution pH, the peak potential for reduction of adsorbed Th-CV complex shifts to more negative values. Measurement of the peak potential for CV and Th CV shows that the peak separation increases with pH. Maximum adsorption of the Th-CV complex attains at pH 4.04. Moreover, the dependence of the peak current of adsorbed Th(IV)-CV on the accumulation potential, preconcentration time and the concentration of acetate was tested in order to optimize the condition for determination of thorium. The effect of accumulation potential on the height of the peak current of Th(IV)-CV was investigated and it is revealed that the optimum accumulation potential is 0.35 V. The adsorption peak for Th(IV)-CV is expected to be dependent upon the adsorption time. It grows with time to a limiting value and then levels off. Obtained data shows that the optimum preconcentration time is 30 s. The Th(IV)-CV peak current decreases with increasing the concentration of acetate. This is probably due to the competitive complexation of Th(IV). The recommended buffer concentration of 20 mM acetate represents a compromise between a need for sufficient buffer capacity and good sensitivity.

Other optimised conditions for the analytical purposes of Th(IV) were examined. It is found that the peak current increases with an increase in the CV concentration up to $2.07 \mu\text{M}$, above which it starts to decline. Therefore, $2.07 \mu\text{M}$ CV was selected. Moreover, the effect of Th(IV) concentration on the peak current was also studied. It is evident that, for a 50 ng ml^{-1} thorium solution, the longer the precon-

tration time, the more metal complex is adsorbed on the electrode surface and the larger is the peak current. As a result, excellent peak-to-background characteristics are obtained, which permit convenient measurements of nanomolar concentrations. The effects of the pulse amplitude and the frequency on the peak height and half-width were also studied. For the optimum sensitivity and a better defined peak, a pulse amplitude of 25 mV and a frequency of 100 Hz were chosen.

Analytical determination of Th(IV)

Examination of the above data, indicates that the optimum conditions for the analytical determination of Th(IV) by SW-ACSV at HMDE are as follows: accumulation time 30 s, accumulation potential -0.35 V, pH 4.04, SW height 25 mV, frequency 100 Hz and the presence of 2.07×10^{-6} mol dm⁻³ catechol violet. The peak height response, under these conditions, as a function of Th(IV) concentration is linear over the range 50-600 nM dm⁻³ Th(IV) at the three peak potentials, E_p , of 0.630, -0.672 and 0.750. The calibration curve is no longer linear, for concentrations beyond the above range. However, higher Th(IV) concentration should be diluted to bring them within the recommended concentration range, or alternatively, shorter deposition time may be used. Using standards prepared from the standard Th(IV) solution, the method gave a linear calibration curve over the range 50-600 nM Th(IV). The slopes of the calibration lines (sensitivity) were 1.06, 1.14 and 1.26 nA/nM/30s with correlation coefficients of 0.996, 0.999 and 0.998, respectively. From the formula $DL = r_d S/b$, the detection limit(DL) was estimated by use of signal-to-noise ratio, r_d , pooled standard deviation, S , and the slopes of calibration, b . The standard deviation of the signal for eight replicate analysis was ± 0.36 nA, giving a detection limit of 1.02, 0.95 and 0.86 nM, for the first, second and third waves, respectively, based on $r_d = 3.0$.

A number of metal ions and anions were tested for interference in the determination of Th(IV), under the experimental conditions described earlier. The interference was performed using 1.0 nM of catechol violet with 0.1 nM Th(IV), with addition of various metal ions. Some of these metal ions were found to form CV complexes that could be adsorbed and reduced on the HMDE. CV complexes of Cu(II), Pb(II) and Ce(IV) were more readily reduced than CV itself, while CV complexes of Cr(VI), Ni(II) and Al(III) were reduced at potentials more negative than that for CV. Thus these metal ions do not interfere with Th(IV)-CV complex. Furthermore, the addition of U(VI) and V(V) gave peaks overlapping those ones with one for Th(IV)-CV complex. Thus U(VI) and V(V) interfere and the peak current for Th(IV)-CV complex decreases due to adsorption competition. Moreover, an electrochemically inactive ions such as Na⁺, K⁺, as well as most commonly occurring anions do not also interfere with the determination of thorium.

Experimental

Reagents and Solutions

Catechol violet, rare earth nitrates of U and Th, interfering

metal nitrates and anion salts of analytical grade purity were used. Stock solutions of fresh 1.0 mmol dm⁻³ in triply distilled water were prepared for the metal ions, anions and CV and were diluted as required for standard solutions. The rare earth solutions were standardized chelatometrically. Acetic acid-sodium acetate buffer solutions were prepared from analytical grade chemicals.

Instrumentation

Electrochemical experiments were carried out on an EG & G PAR Potentiostat/Galvanostat model 363A. An EG&G three electrodes electrolysis cell system model SMDE 303A was used. A hanging mercury drop electrode (HMDE) in the medium hanging drop mode was used as the working electrode. The electrode area was 1.51×10^{-2} cm². Platinum wire and silver/silver chloride/aqueous saturated potassium chloride electrodes were used as counter and reference electrodes, respectively. The electrochemical system was interfaced with an IBM Value Point 433 DX/DP Computer. The data were acquired, stored, and manipulated employing EG&G M270/500 software which controls the potentiostat via IEEE 488 GPIB. Positive feedback was used for compensation of the solution resistance. All solutions were freshly prepared and kept under nitrogen atmosphere. Solutions were purged with pure nitrogen before the measurements, and pure nitrogen was maintained above the working solution. The cyclic voltammograms and chronoamperograms were recorded in equally spaced time intervals both for the pure supporting electrolyte solution and in the presence of the substrate. The background data were subtracted digitally implying the assumption of a simple additivity of faradic and non-faradic currents, minimizing effects such as double layer charging currents.

For square-wave experiments, Th(IV)-CV complex characterization, calibration and determination of Th(IV) measurements, the electrochemical analyzer was operated at a square-wave frequency, f , of 100 Hz. The maximum sensitivity in SWV should be obtained for a maximum value of τ corresponding to a frequency of 100 Hz and square-wave amplitude of 25 mV.

Procedure

All measurements were obtained at 298 ± 0.1 K. To produce adsorptive cyclic voltammograms and chronoamperograms a 10 cm³ analyte solution in the reagent 20 mM acetic acid-sodium acetate solution was used. Solutions were deaired by purging with pure nitrogen. After formation of a new HMDE drop at a deposition potential of 0.35 V, the solution was stirred for 30 sec (accumulation time) and equilibrated for 5 sec. A negative potential scan was recorded using the cyclic voltammetric and chronoamperometric modes

References

1. S. Raheem and K. M. M. K. Prasad, *Talanta*, **40**, 1809 (1993).
2. K. M. M. K. Prasad and S. Raheem, *Microchim. Acta*, **112**, 63 (1993).
3. J. R. Kramer, J. Gleed and K. Gracey, *Anal. Chim. Acta*, **284**, 599

- (1994).
4. K. M. M. K. Prasad, P. Vijayalekshmi and C. K. Sastri, *Analyst*, **119**, 2817 (1994).
 5. W. D. Wakley and L. P. Varga, *Anal. Chem.*, **44**, 169 (1972).
 6. J. Kobayashi, M. Baba and M. Miyazaki, *Anal. Sci.*, **10**, 287 (1994).
 7. B. Fairman, A. Sanzmedel, M. Gallego, M. J. Quintela, P. Jones and R. Benson, *Anal. Chim. Acta*, **286**, 481 (1994).
 8. D. J. Hawke and H. K. J. Powell, *Anal. Chim. Acta*, **299**, 257 (1994).
 9. L. F. Capitanvallvey, M. C. Valencia and G. Miron, *Anal. Chim. Acta*, **289**, 365 (1994).
 10. D. V. Vukomanovic and G. W. Vanloon, *Fresenius, J. Anal. Chem.*, **350**, 352 (1994).
 11. R. B. Zhn, J. L. Han and H. Y. Chen, *Chem. J. Chinese Univ.-Chin.*, **16**, 35 (1995).
 12. R. Abdel-Hamid, *J. Chem. Soc. Perkin Trans. 2*, 691(1996).
 13. H. M. El-Sagher, *Monatscheffe fur Chemie*, **130**, 295 (1999).
 14. R. Abdel-Hamid, H. M. El-Sagheir and M. K. Rabia, *Can. J. Chem.*, **75**, 162 (1997).
 15. J. C. K. Placers, M. T. S. Alacjos and F. J. G. Montelonge, *Talanta*, **39**, 649 (1992).
 16. D. V. Vukomanovic, J. A. Page and G. W. Vanloon, *Can. J. Chem.*, **69**, 1418 (1991).
 17. D. V. vukomanovic and G. W. Vanloon, *Talanta*, **41**, 387 (1994).
 18. Jr. D. K. Gosser "Cyclic Voltammetry, Simulation and Analysis of Reaction Mechanism", VCH, New York, (1993).
 19. B. H. Wopschall and I. Shain, *Anal. Chem.*, **39**, 1514 (1967).
 20. B. H. Wopschall and I. Shain, *Anal. Chem.*, **39**, 1534 (1967).
 21. E. Laviron, *Electroanal. Chem.*, **12**, 53 (1982).
 22. A. J. Bard and L. R. Faulkner, "Electrochemical Methods, Fundamentals and Applications" Wiley, New York, (1980).
 23. B. Janik and P. J. Elving, *J. Electrochem. Soc.*, **116**, 1089(1965).
 24. M. P. Soriage and A. T. Hubbard, *J. Am. Chem. Soc.*, **104**, 3937 (1982).
 25. F. C. Anson, *Anal. Chem.*, **38**, 54 (1966).
 26. K. Ogura and K. Arinoba, *J. Electroanal. Chem.*, **89**, 175 (1978).
 27. K. Ogura, K. Seneo, S. Murakami and T. Yoshino, *J. Inorg. Nucl. Chem.*, **42**, 1165 (1980).
 28. K. Ogura, Y. Fushima and I. Aomizu, *J. Electroanal. Chem.*, **107**, 271 (1980).
 29. M. Jarosz, *Analyst*, **111**, 681(1986).
 30. D. D. Perrin, Ed., "Stability constants of metal ion complexes". Part B. Organic Ligands. IUPAC Chemical Data Series, No. **22**. Pergamon Press Ltd: 1979.